Loo, S., & Erman, J. E. (1975) *Biochemistry 14*, 3467–3470.
Loo, S., & Erman, J. E. (1977) *Biochim. Biophys. Acta 481*, 279–282.
Mannervik, B. (1983) *Contemporary Enzyme Kinetics and Mechanism* (Purich, D. L., Ed.) pp 75–95, Academic Press, New York.
Margoliash, E., & Frohwirt, N. (1959) *Biochem. J. 71*, 570–572.
Nicholls, P., & Mochan, E. (1971) *Biochem. J. 121*, 55–67.
Satterlee, J. D., Moench, S. J., & Erman, J. E. (1987) *Biochim. Biophys. Acta 912*, 87–97.
Sivaraja, M., Goodin, D. B., Smith, M., & Hoffman, B. M. (1989) *Science 245*, 738–740.
Spangler, B. D., & Erman, J. E. (1986) *Biochim. Biophys. Acta 872*, 155–157.
Summers, F. E., & Erman, J. E. (1988) *J. Biol. Chem. 263*, 14267–14275.
Vitello, L. B., & Erman, J. E. (1987) *Arch. Biochem. Biophys. 258*, 621–629.
Vitello, L. B., Huang, M., & Erman, J. E. (1990) *Biochemistry 29*, 4283–4288.
Yandell, J. K., & Yonetani, T. (1983) *Biochim. Biophys. Acta 748*, 263–270.
Yonetani, T. (1965) *J. Biol. Chem. 240*, 4509–4514.
Yonetani, T., Schleyer, H., & Ehrenberg, A. (1966) *J. Biol. Chem. 241*, 3240–3242.

Steady-State Fluorescence and Time-Resolved Fluorescence Monitor Changes in Tryptophan Environment in Arginase from *Saccharomyces cerevisiae* upon Removal of Catalytic and Structural Metal Ions

Susan M. Green,[‡,§] Jay R. Knutson,[∥] and Preston Hensley*[,‡]

Department of Biochemistry and Molecular Biology, Georgetown University, Washington, D.C. 20007, and Laboratory of Technical Development, National Heart, Lung and Blood Institute, National Institutes of Health, Bethesda, Maryland 20892

Received April 27, 1990

ABSTRACT: Yeast arginase is a trimeric protein of identical subunits, each containing three tryptophans. Time-resolved fluorescence and steady-state fluorescence were employed to monitor the effects of removing the weakly bound catalytic Mn^{2+} as well as the tightly bound structural Zn^{2+}/Mn^{2+}. Resolution of the total native emission spectrum into decay-associated spectra (DAS) yielded components with lifetimes of 0.1, 1.2, and 4.0 ns. Upon removal of the catalytic metal, the intensities increased ~20% while the lifetimes increased <10%, and the DAS were unchanged except in intensity. The two major components are well resolved, but the 0.1-ns term is small and dominated by scattered excitation. In contrast, removal of the structural metal increased decay times to 0.2, 1.8, and 5.3 ns. More important, both native DAS red-shifted and became indistinguishable. These data suggest that removal of the catalytic metal does little to change the microenvironments of the individual tryptophans while removal of the structural metal causes partial unfolding of the protein. The excitation spectra for the active and inactive trimers were resolved into their excitation DAS (IEDAS), suggesting ground-state heterogeneity of the fluorescent species. In contrast, the excitation spectra of arginase without the structural metal could not be resolved due to the indistinguishable DAS. The tryptophans are quenched by acrylamide but not by cesium or iodide. Global analysis of the acrylamide quenching data resulted in two quenching decay-associated spectra (QDAS) which correlated well with the DAS. Since the apoenzyme does not exhibit tryptophan accessibility to either positive or negative ionic quenchers, one must assume that the "unfolded" monomeric protein retains considerable tertiary structure.

Arginase (EC 3.5.3.1) from *Saccharomyces cerevisiae* catalyzes the first committed step in the degradation of L-arginine, hydrolyzing it to L-ornithine and urea. In yeast, as opposed to higher eukaryotes, arginase and ornithine transcarbamylase (OTCase)[1] (EC 2.1.3.3), which catalyzes the first committed step in the biosynthesis of L-arginine, both exist in the cytoplasm. Thus, one common mechanism for urea cycle regulation, namely, compartmentalization, is nonexistent in yeast. Therefore, yeast have adopted another mode of regulation in the form of a multienzyme complex between OTCase and arginine. In this complex, OTCase and arginase associate one-to-one, and OTCase activity is inhibited while arginase remains active. This system was first characterized by Wiame and co-workers (Bechet & Wiame, 1965; Messenguy & Wiame, 1969; Wiame, 1971; Penninckx et al., 1974; Penninckx, 1975; Penninckx & Wiame, 1976) and subsequently studied in our laboratory (Eisenstein et al., 1984, 1986;

* Address correspondence to this author at the Macromolecular Sciences Department, SmithKline and Beecham Pharmaceuticals, P.O. Box 1539, King of Prussia, PA 19406-0939.
‡ Georgetown University.
§ Present address: Department of Biological Chemistry, The Johns Hopkins University, School of Medicine, 725 N. Wolfe St., Baltimore, MD 21205.
∥ National Institutes of Health.

[1] Abbreviations: OTCase, ornithine transcarbamylase; Hepes, 4-(2-hydroxyethyl)-1-piperazineethanesulfonic acid; DAS, decay-associated spectra; IEDAS, indirect excitation decay-associated spectra; QDAS, quenching decay-associated spectra.

0006-2960/90/0429-9159$02.50/0

Eisenstein, 1985; Duong et al., 1986; Eisenstein & Hensley, 1986; Hensley, 1988).

It has been previously shown that metals play an important role in the maintenance of the catalytic activity and the stabilization of the tertiary and quaternary structure of arginase from *Saccharomyces cerevisiae* (Hirsch-Kolb & Greenberg, 1968; Hirsch-Kolb et al., 1970, 1971; Carvajal et al., 1971, 1977, 1978; Vielle-Breitburd & Orth, 1972; Stewart & Caron, 1977; Eisenstein, 1985; Green et al., 1988, 1990a,b; Green, 1989). We have shown that removal of the catalytic Mn^{2+} by dialysis results in the reversible loss of enzymatic activity (Green et al., 1990a) while removal of the structural Zn^{2+}/Mn^{2+} by dialysis with EDTA results in decreases in both the ellipticity and sedimentation coefficients (Green et al., 1990a). Structural Zn^{2+}/Mn^{2+} removal destabilizes the trimer, resulting in a reversible monomer–trimer equilibrium (Green et al., 1990b).

Steady-state fluorescence experiments also demonstrated large changes upon removal of metal ions from arginase (Green et al., 1990b). Removal of the catalytic Mn^{2+} alone results in a 30% increase in fluorescence intensity without a change in the wavelength maximum of 337 nm. Removal of the structural Zn^{2+}/Mn^{2+} results in an increase of >100% and a red-shift of 15 nm from the native spectrum. Since arginase has three tryptophans per polypeptide chain (Sumrada & Cooper, 1984), time-resolved fluorescence experiments were undertaken to characterize these changes in terms of multiple fluorescent species using the global approach described in the Brand laboratory (Beechem et al., 1983; Knutson et al., 1983).

Experimental Procedures

Materials. 4-(2-Hydroxyethyl)-1-piperazineethanesulfonic acid (Hepes)[1] was purchased from U.S. Biochemicals. $MnCl_2$, melatonin, and EDTA were purchased from Sigma. All other chemicals were reagent grade.

Methods. Arginase was purified from *Saccharomyces cerevisiae* strain 02232i as previously described (Green et al., 1990a). Arginase concentration was determined from the specific absorbance coefficient $A_{279nm} = 0.71$ cm^2 mg^{-1} (Eisenstein, 1985). The inactive enzyme was made by dialysis overnight at 4 °C against 20 mM Hepes, pH 7.0, and 200 mM NaCl containing no exogenous Mn^{2+}. Removal of the structural metal ion was achieved by extended dialysis against the same buffer containing 1 mM EDTA or incubation with 5 mM EDTA for approximately 2 h at 30 °C (Green et al., 1990b). Arginase is stable at this temperature (Green et al., 1990a).

Decay-associated spectra (DAS) (Knutson et al., 1982) were obtained from the simultaneous analysis of decay curves taken at 5-nm intervals across the emission band (global analysis) using a laser-based instrument described elsewhere (Knutson, 1988). The light source is a synchronously pumped, cavity-dumped dye laser which provides <20-ps pulses at 295 nm with a repetition rate of 4 MHz and an average power of approximately 200 μW. These vertically polarized pulses are obtained by frequency doubling of horizontally polarized, visible dye laser pulses. They were rotated from their original polarization by a Babinet–Soleit compensator. The final UV polarization establishes a vertical symmetry axis. Hence, all total intensity decay measurements were obtained through an emission sheet polarizer oriented 55° from that axis [magic angle; for a review, see Badea and Brand (1979)]. Emission was selected by computer-controlled JYH10 monochromators with the bandwidth set at 8 nm and a 3-mm glass slide added to further reject stray excitation. Decay curves were obtained by time-correlated single photon counting using Ortec NIM modules and a Tracor Northern 1710 MCA under computer control (Knutson, 1988). Data were transferred to a HP1000:A900 minicomputer for subsequent global analysis.

For decay curve analysis, it was possible, in many cases, to nullify the effects of small artifacts due to stray light and/or color shift errors by introducing a small, fixed-lifetime component (T circa 90 ps). This method has been shown to be as effective as more rigorous corrections when the errors are not too large and the terms' lifetime, T, obeys $\Delta t_{channel} = T \ll W$, where W is the width of the instrument response function (Knutson, 1987). The R955 photomultiplier operated with a time spread (half-width) of ca. 900 ps in these experiments. With rigorous color correction, this arrangement can resolve lifetimes as short as 100 ps (Knutson et al., 1984). Below that range, a faster detector is required.

Anisotropy decay curves were obtained by alternating collection of parallel (0° from vertical) and perpendicular (90°) emission for 20-s intervals until each curve peak exceeded 1.2×10^4 counts (ca. 200 s). The G factor (Chen & Bowman, 1965) was measured with an aqueous solution of melatonin, whose lifetime (circa 5.5 ns) far exceeds its rotational correlation time (circa 200 ps) by alternating collection between parallel and perpendicular emission as described above. This material also served as a color shift standard. For some measurements, G was reduced to unity with a wedge depolarizer (Optics for Research, DPU) carefully placed in the entrance slit of the monochromator. Analysis was by both "sum and difference" (Dale et al., 1977; Knutson et al., 1986; Davenport et al., 1986b) and global (Beechem et al., 1985) methods.

Indirect excitation decay-associated spectra (IEDAS) were obtained from a matrix inversion approach (Knutson et al., 1982a; Brand et al., 1985; Sackett et al., 1990; Knutson et al., unpublished experiments).

Steady-state spectra were obtained by using the photon counting mode of an ISS-Greg 200 spectrophotofluorometer with an R6G quantum counter in the reference channel. Spectra were not corrected for monochromator blaze or detection sensitivity, and bandwidths of 8 nm were used (2-mm slits). Quenching decay-associated spectra (QDAS) were obtained by global analysis of the surface (intensity versus wavelength and quencher concentration) for a sum of Stern–Volmer processes. Algorithms for each process are available from the authors on request.

Results

Fluorescence decay curves of arginase were recorded as a function of wavelength throughout the emission spectrum. Figure 1 shows the fit to the decay curves determined by global analysis (Beechem et al., 1983; Knutson et al., 1983) as well as the residuals and autocorrelation of the fit for arginase in the presence of exogenous Mn^{2+} (A), in the absence of Mn^{2+} (B), or dialyzed against EDTA (C). The data were best described by three fluorescent species and a fourth short fixed component to compensate for any scattered excitation or color shift. The small magnitude of the residuals and the random autocorrelation demonstrate that the fit is reasonable.

By use of linked analysis, the amplitude associated with each of the fluorescent species can be obtained versus wavelength. Figure 2 is a summary of the relative intensity associated with each of the fluorescent species determined in Figure 1, all recorded at 340 nm. Arginase in the presence of the catalytic Mn^{2+} exhibits fluorescent species with lifetimes of 0.1, 1.2, and 4.0 ns. Removal of the catalytic Mn^{2+} only slightly increases the lifetimes of the fluorescent species to 0.1, 1.3, and 4.3 ns. Removal of the structural metal by EDTA, however,

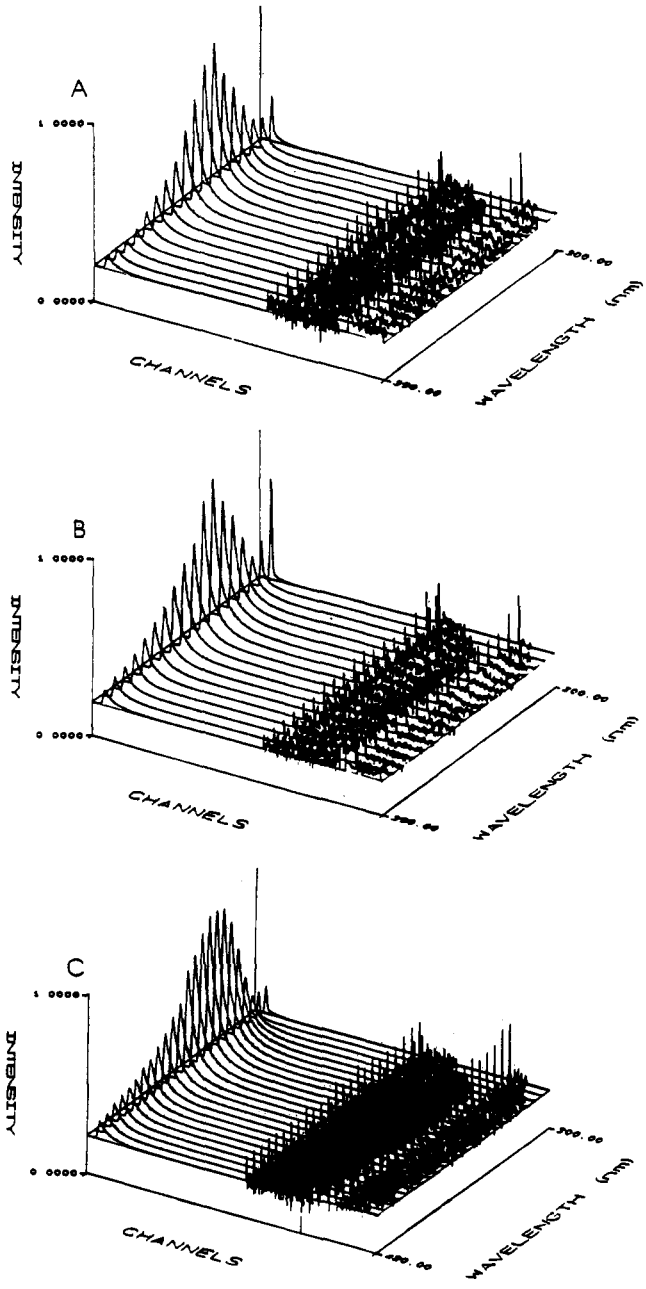

FIGURE 1: Decay surface of arginase. Time-resolved decay curves were measured at 5-nm intervals from 300 to 450 nm in (panel A) 20 mM Hepes, pH 7.0, 200 mM NaCl, and 1 mM $MnCl_2$; (panel B) 20 mM Hepes, pH 7.0, and 200 mM NaCl; or (panel C) 20 mM Hepes, pH 7.0, 200 mM NaCl, and 1 mM EDTA. Shown is the decay followed by the residuals and the autocorrelation of the fit at each wavelength. Arginase concentration was 0.1 mg mL^{-1}.

yields lifetimes of 0.2, 1.8, and 5.3 ns. In all three cases, the intensity of the long-lifetime species is the highest. Furthermore, the intensity associated with each species increases upon removal of metal ions, similar to that shown previously for the intensity of the steady-state emission spectra (Green et al., 1990b).

The total time-resolved fluorescence emission spectra for each sample was resolved into contributions from each decay-associated spectrum (DAS) (Knutson et al., 1982) as shown in Figure 3. The total spectrum is denoted by a solid line. The intensity of the DAS associated with the long-lifetime species is denoted with the dashed–dotted line, while the DAS for the middle lifetime species is denoted by the dashed line. In all samples, the apparent short-lifetime species is small and partially obscured by contributions from scattered

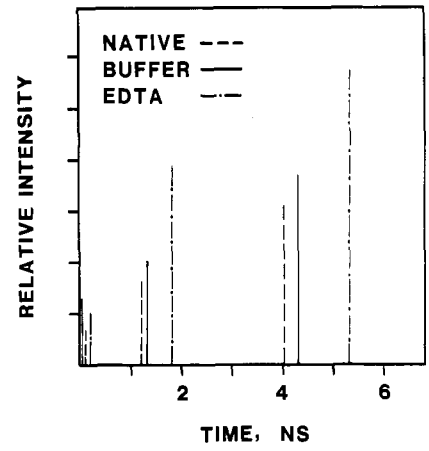

FIGURE 2: Comparison of the intensities of the fluorescent species of arginase at 340 nm. The relative intensity and lifetime of each of the fluorescent species are shown. Arginase was dialyzed against 20 mM Hepes, pH 7.0, 200 mM NaCl, and 1 mM $MnCl_2$ (dashed line); 20 mM Hepes, pH 7.0, and 200 mM NaCl (solid line); and 20 mM Hepes, pH 7.0, 200 mM NaCl, and 1 mM EDTA (dashed–dotted line).

(Rayleigh and Raman) excitation, as shown by the dotted line. Thus, only two lifetime species were reliably resolved with this detection system. It is evident here that the intensity of the long-lifetime species is the most prevalent in all three samples.

A shift in emission maximum of DAS is most apparent if the spectra are peak-normalized. A comparison of peak-normalized DAS for the middle lifetime species (Figure 4A) shows that both native and inactive trimeric enzymes have DAS that are nearly superimposable, suggesting little change in tryptophan environment upon removal of the catalytic Mn^{2+}. In contrast, the red-shift of the DAS for the EDTA-treated enzyme suggests the movement of the tryptophans in this sample to more polar environments. A comparison of DAS for the long-lifetime species (Figure 4B) demonstrates similar results for all three samples: the two trimeric forms of the enzyme have DAS that are superimposable, while the apoenzyme has DAS that are red-shifted, again indicative of exposure of the tryptophan residues to more polar environments.

Since the shapes and wavelength maxima of the middle and long lifetime fluorescent species' DAS appear very similar, it was desirable to compare the DAS of the middle species with that of the long species for each sample to ascertain if the two are distinguishable. Figure 5 shows the results of this comparison. Native arginase and inactive, trimeric arginase have middle and long DAS that are easily separated from each other with emission maxima of 335 and 342 nm, respectively (Figure 5A,B). For arginase dialyzed against EDTA, however, both DAS red-shift to 354 nm and become indistinguishable (Figure 5C).

A distribution fit of the data was conducted for comparison (Alcala et al., 1987a–c). When one fits for a Gaussian distribution of lifetimes in the absence of global linkage, the result is a very broad, ill-determined peak. Such an analysis is shown in Figure 6A for arginase in the presence of exogenous Mn^{2+} at 340 nm. This broad curve shifts erratically with emission wavelength, tending generally toward longer lifetimes in the red (data not shown). Through global linkage (testing agreement at all wavelengths), however, one obtains two sharp peaks that are well separated and centered around the discrete lifetimes determined above (Figure 6B).

If the DAS for the two species have distinct emission maxima, or if the shape of the DAS is different, the ratio of the long relative to that of the middle species will be different

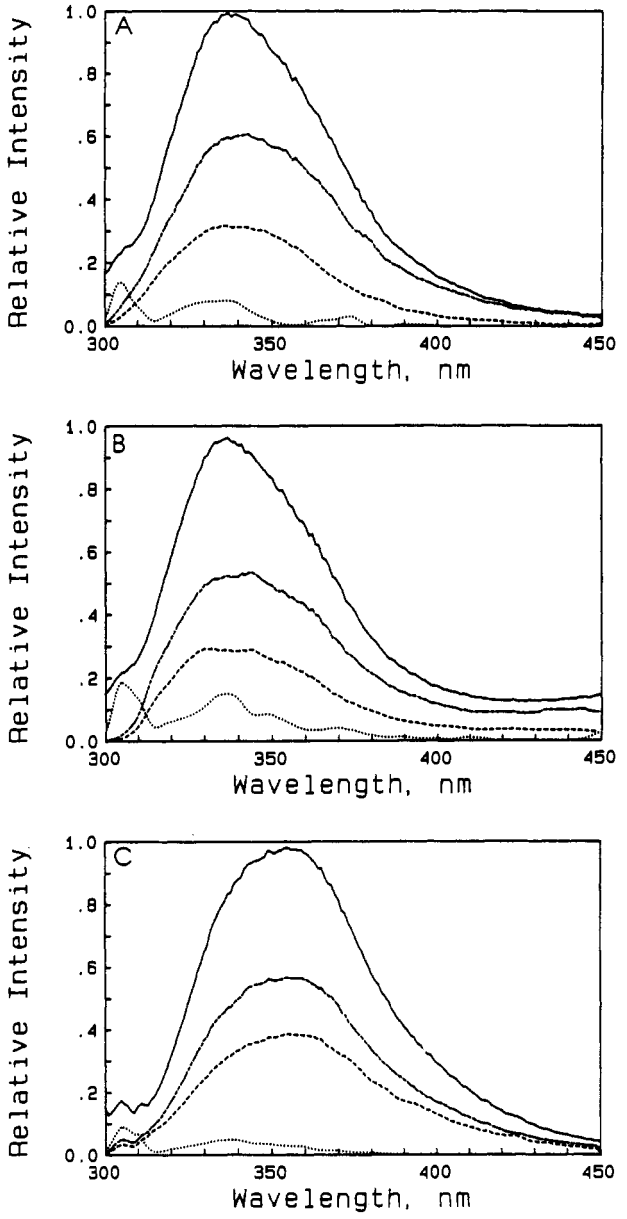

FIGURE 3: Resolution of the total fluorescent spectrum into the decay-associated spectra (DAS). The total spectrum is denoted by the solid line, the intensity associated with the long-lifetime component by the dashed–dotted line, the intensity associated with the middle component by the dashed line, and the intensity associated with the short-lifetime species by the dotted line. Panel A shows arginase that was dialyzed against 20 mM Hepes, pH 7.0, 200 mM NaCl, and 1 mM $MnCl_2$. Panel B shows arginase dialyzed against 20 mM Hepes, pH 7.0, and 200 mM NaCl, and panel C shows arginase dialyzed against 20 mM Hepes, pH 7.0, 200 mM NaCl, and 1 mM EDTA.

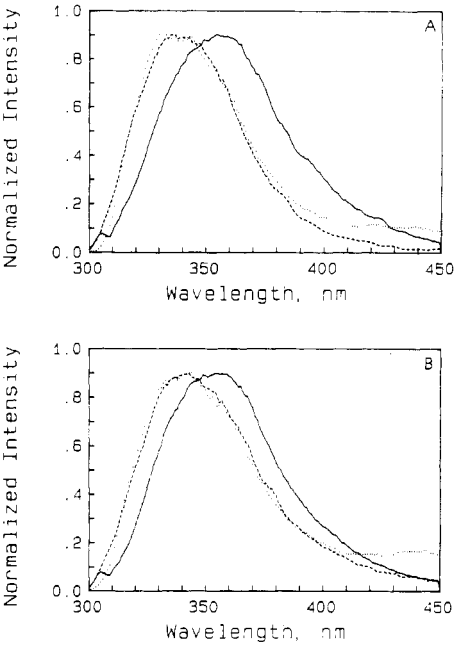

FIGURE 4: Comparison of the middle- and long-lifetime components for each sample. Arginase in $MnCl_2$ is denoted by the dashed line; arginase without the catalytic Mn^{2+} is denoted by the dotted line. Arginase in EDTA is shown by the solid line. Panel A shows the comparison of peak-normalized DAS for the middle-lifetime components. Panel B shows the comparison of peak-normalized DAS for the long-lifetime components.

Table I: Analysis of Dynamic Quenching Data for Arginase

sample[a]	quencher	K_{sv1}[b]	% I_1[c]	K_{sv2}	% I_2
arginase, 1 mM $MnCl_2$	acrylamide	0.88	66	4.35	34
	KI	0.14	94	3.33	05
	CsCl	0.24	100		
arginase, dialyzed	acrylamide	0.55	49	2.44	51
	KI	0.00	73	3.59	27
	CsCl	0.11	100		
arginase, 1 mM EDTA	acrylamide	1.26	59	5.96	41
	KI	0.08	88	5.33	12
	CsCl	0.03	100		

[a] Arginase was dialyzed overnight at 4 °C against 20 mM Hepes, pH 7.0, and 200 mM NaCl as described in the table. [b] Stern–Volmer constants were calculated by using global linkage (Knutson et al., 1983; Beechem et al., 1983). [c] Intensities were calculated at 340 nm.

at each emission wavelength. Excitation spectra taken at these emission wavelengths must also be differing mixtures. When the mixing ratios and excitation spectra at two such emission wavelengths are used, the (indirect) excitation decay-associated spectra (IEDAS) (Knutson et al., 1982a; Brand et al., 1985; Sackett et al., 1990; Knutson et al., unpublished results) can also be resolved as described under Experimental Procedures. Since the two trimeric forms of the enzyme have DAS that are easily separated, two IEDAS can be directly separated. This is shown in Figure 7A,B. The presence of two different IEDAS demonstrates ground-state heterogeneity of the fluorescent species, indicating different environments around the three tryptophans. This is shown by the wavelength maxima for the native and inactive trimeric enzymes of 286 and 292 nm and 284 and 292 nm, respectively. This method, however, is not applicable for the enzyme that had been treated with EDTA (Figure 7C). Due to numerical instability of matrix inversion when DAS are indistinguishable (and the ratio of the intensities of the two species is nearly the same at every wavelength), there are large errors associated with these two IEDAS, resulting in the same overall shape.

Dynamic quenching experiments were undertaken to determine if arginase in the three states of metal ligation demonstrates different quenchabilities to various small molecules. The results of these studies are given in Table I as Stern–Volmer constants (and percent intensity associated with each constant) for three quenchers: acrylamide, KI, and CsCl. When arginase was quenched with acrylamide, two Stern–Volmer constants were obtained for each sample, one demonstrating low quenchability with a K_{sv} of approximately 1 and one demonstrating higher quenchability with a K_{sv} between 2.44 for the inactive trimeric enzyme and 5.96 for the apoenzyme. These constants were both associated with a significant intensity in all three cases, varying from 49% to 66% for the species having the lower quenchability. CsCl, a positive ionic quencher, was not an effective quencher in arginase as shown by very low Stern–Volmer constants. KI, a negative

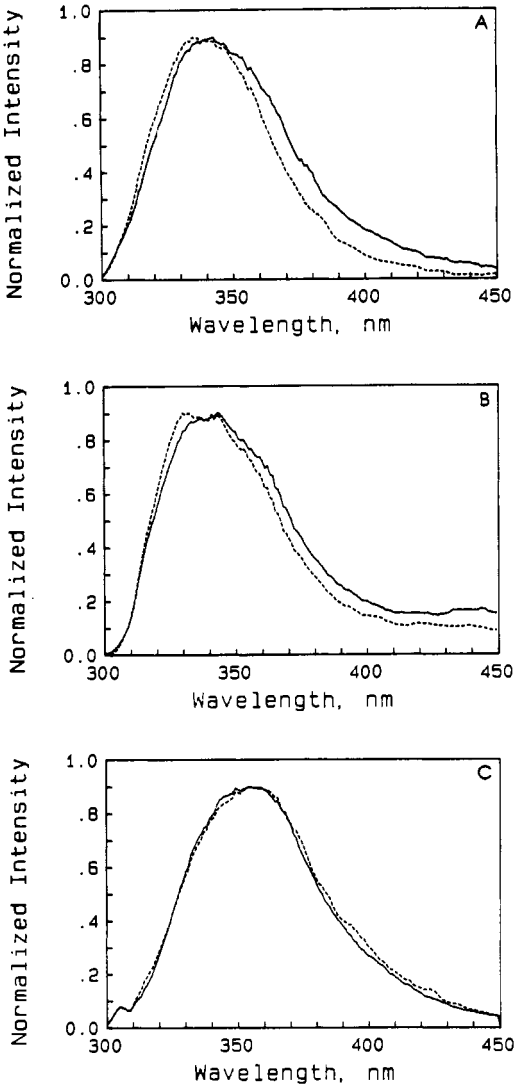

FIGURE 5: Comparison of the middle-lifetime component with the long-lifetime component in each sample. The middle-lifetime component is denoted by the dashed line, and the long lifetime is denoted by the solid line. Arginase in $MnCl_2$ is shown in panel A. Panel B shows arginase in the absence of the weakly associated Mn^{2+}, and panel C shows arginase in EDTA.

ionic quencher, had only a marginal effect on all samples; the majority of the total fluorescence was not quenched by KI as demonstrated by K_{sv}'s of approximately 0.1. The differences in susceptibility to the three quenchers are shown in Stern–Volmer plots as F_0/F in Figure 8. As illustrated, the fluorescence decreases significantly upon the addition of acrylamide to arginase, particularly in the apoenzyme (panel A), while there is little change in fluorescence upon the addition of either KI (panel B) or CsCl (panel C) to any of the three samples.

Just as DAS can be derived from the surface of intensity versus wavelength and time, quenching decay-associated spectra (QDAS) can be extracted from inversion methods and/or global analysis of the surface: intensity versus wavelength and concentration (Knutson et al., 1982a; Brand et al., 1985). The QDAS derived from acrylamide quenching are shown in Figure 9 and compared to the DAS obtained previously. As in Figure 5, the middle-lifetime DAS is denoted by the dashed line and the long-lifetime DAS by the solid line. The QDAS for the less accessible species to acrylamide is represented by the squares, and the QDAS for the more accessible species is represented by the triangles. As with the DAS, the QDAS for the native enzyme and the inactive,

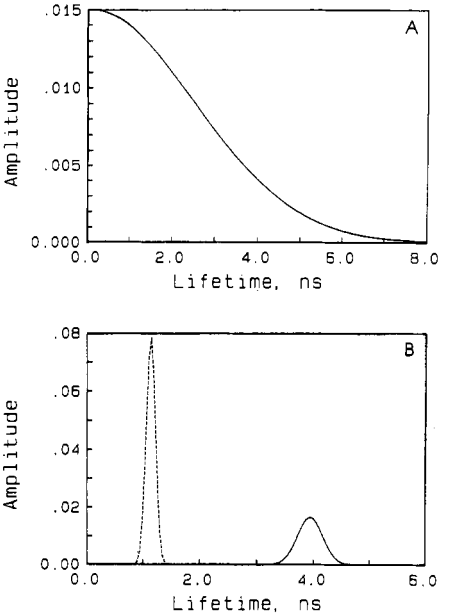

FIGURE 6: Distribution fit of the lifetimes for arginase in $MnCl_2$. Panel A shows the results of a fit for a Gaussian distribution of the lifetimes for arginase in the presence of $MnCl_2$ in the absence of global linkage at 340 nm. Panel B shows the results of the same fit using global linkage analysis. The middle-lifetime component is denoted by the dashed line, and the long-lifetime component is denoted by the solid line.

Table II: Collision Rates of Arginase Quenched with Acrylamide

sample[a]	k (ns^{-1} M^{-1})[b]
arginase, 1 mM $MnCl_2$	0.73, 1.09
arginase, dialyzed	0.42, 0.57
arginase, 1 mM EDTA	0.68, 1.12

[a] Arginase was dialyzed overnight against 20 mM Hepes, pH 7.0, and 200 mM NaCl as described in the table. [b] The collision rate, k, was determined by dividing the two Stern–Volmer constants for arginase, quenched with acrylamide, by their corresponding lifetimes.

trimeric enzyme are clearly separate, while the QDAS red-shift and become almost indistinguishable upon removal of the structural Zn^{2+}/Mn^{2+}. More importantly, the acrylamide QDAS correlate well with the DAS in terms of wavelength maximum and overall width, which suggests the identification of acrylamide quenching constants with specific lifetimes. In all three samples, the species less quenched by acrylamide has the shorter lifetime, and the more highly quenched species has the higher lifetime. The QDAS for arginase without catalytic manganese are irregularly shaped, but the overall features are similar to the DAS.

Since there is some correlation between the acrylamide QDAS and DAS, it is reasonable to estimate k, the bimolecular quenching (collision) rate, for each species (Table II). Native arginase has collision rate constants of 0.73 and 1.09 ns^{-1} M^{-1}, corresponding to the weakly and strongly quenched fluorescent species, respectively. For inactive, trimeric arginase, these rate constants become 0.42 and 0.57 ns^{-1} M^{-1}. Removal of the structural metal returns these values of 0.68 and 1.12 ns^{-1} M^{-1}. Thus, the collision rate constants for the native enzyme and the apoenzyme are nearly identical. In contrast, for the catalytically inactive enzyme, the apparent collision rate constants are half those of the other two samples.

Since the release of the structural metal ion has been shown to result in a reversible monomer–trimer equilibrium, anisotropy experiments were performed to determine if there were differences in the mobility of side chains in the enzyme as a function of metal ligation. The smoothed experimental an-

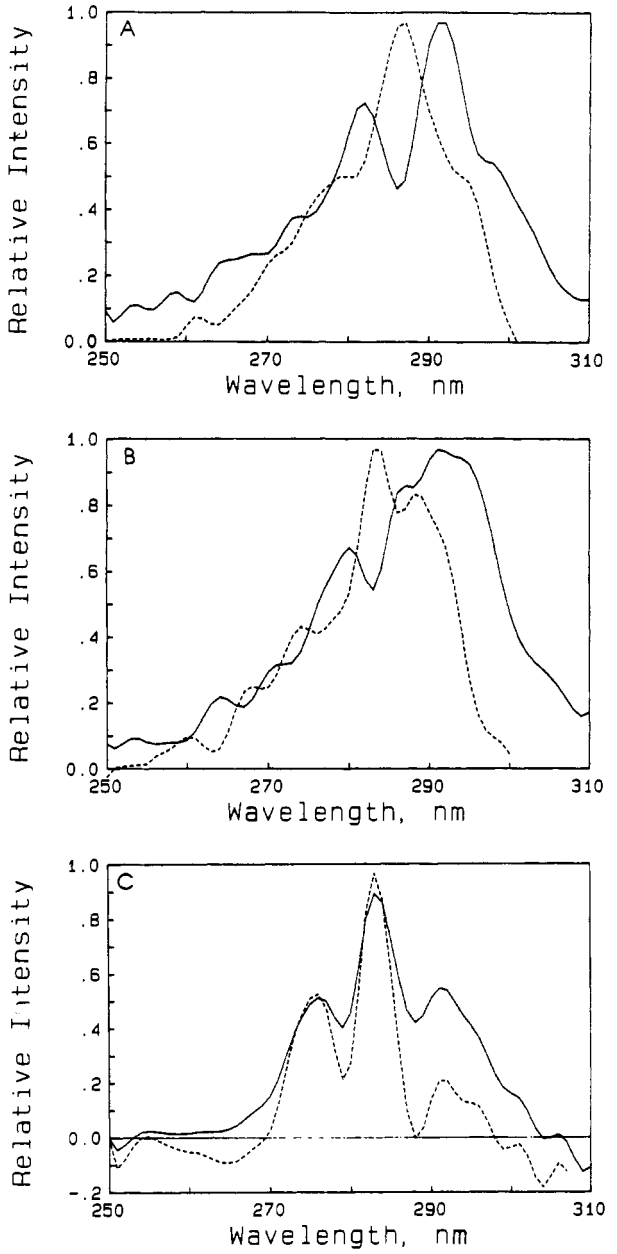

FIGURE 7: Indirect excitation decay-associated spectra for arginase. Panel A shows arginase in the presence of $MnCl_2$; panel B shows arginase in the absence of the catalytic Mn^{2+}; panel C shows arginase in the presence of EDTA. Arginase concentration was 0.12 mg mL^{-1}. The dashed line represents the IEDAS associated with the long-lifetime species. The solid line is the IEDAS associated with the middle-lifetime species. Note that panels A and B show shifts in the wavelength maximum while panel C does not.

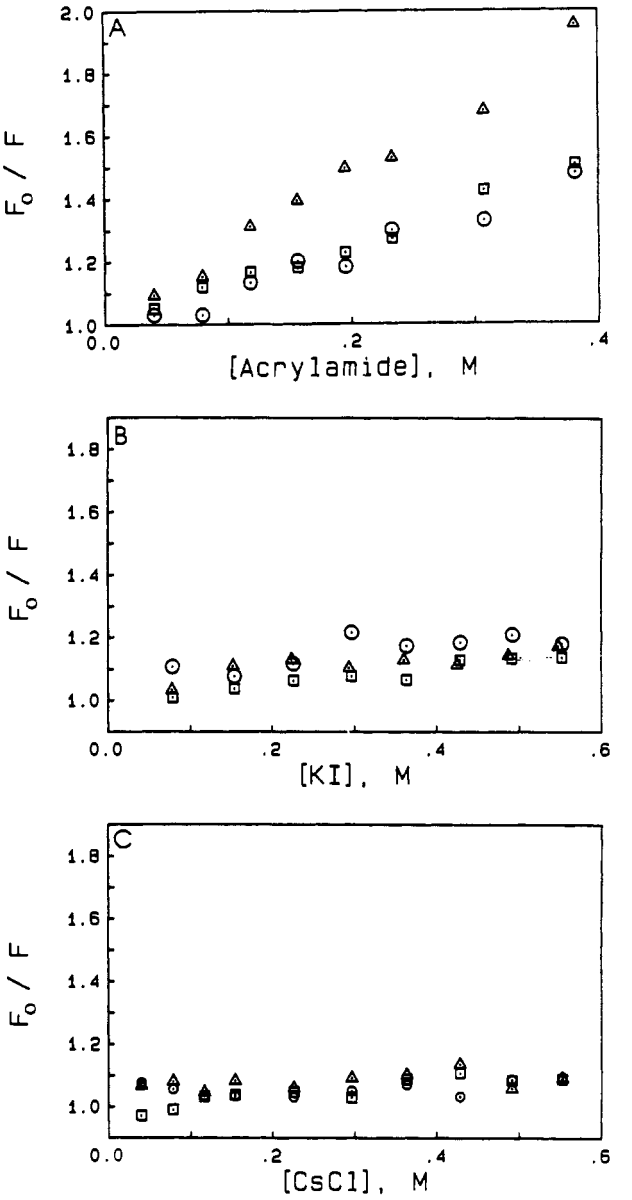

FIGURE 8: Stern–Volmer plots of arginase. Arginase was quenched with 8 M acrylamide (panel A), 4 M KI (panel B), or 4 M CsCl (panel C). Arginase was dialyzed against 20 mM Hepes, pH 7.0, 200 mM NaCl, and 1 mM $MnCl_2$ (squares); 20 mM Hepes, pH 7.0, and 200 mM NaCl (circles); or 20 mM Hepes, pH 7.0, 200 mM NaCl, and 1 mM EDTA (triangles). Excitation was at 295 nm; emission was monitored at 340 nm. Arginase concentration was 0.15 mg mL^{-1}.

isotropies are shown in Figure 10. The data for the two trimeric forms of the enzyme have similar anisotropy curves (top two curves), while the sample that has been treated with EDTA (bottom curve) demonstrates a larger fast component than the other two as seen as a steep descent of the curve in the early channels followed by a component similar to the other two samples in the later channels. A scaled version of the "lamp" (impulse–response) curve is given as reference (dashed–dotted line). The results of these studies are summarized in Table III. As suggested in Figure 10, the steady-state anisotropies for the native and inactive, trimeric arginase are similar with r values of 0.136 and 0.113, respectively. Arginase in EDTA has an overall anisotropy half that of the other two (0.061). Since the shape of the anisotropy curve for arginase in EDTA is different only in the early channels, it suggests an increase in segmental mobility. Sum and difference analyses (Davenport et al., 1986b; Knutson et al., 1986) found that each sample has two rotational correlation times of <1 ns and ~20 ns, called "fast" and "slow" rotation components, respectively. The drop in anisotropy in the apoenzyme occurs because the amplitude of the short, fast component is twice as prevalent (at 40% as compared to 20%) as in the two trimeric forms of the enzyme.

Table III: Anisotropies and Rotational Correlation Times for Arginase

sample[a]	r^b	ϕ (ns)	% amplitude$_{fast}$
arginase, 1 mM $MnCl_2$	0.136	0.08, 19.3	20
arginase, dialyzed	0.113	0.66, 22.0	19
arginase, 1 mM EDTA	0.061	0.74, 18.1	40

[a] Arginase was dialyzed overnight against 20 mM Hepes, pH 7.0, and 200 mM NaCl as described in the table. [b] Anisotropies and rotational correlation times were determined as described under Experimental Procedures.

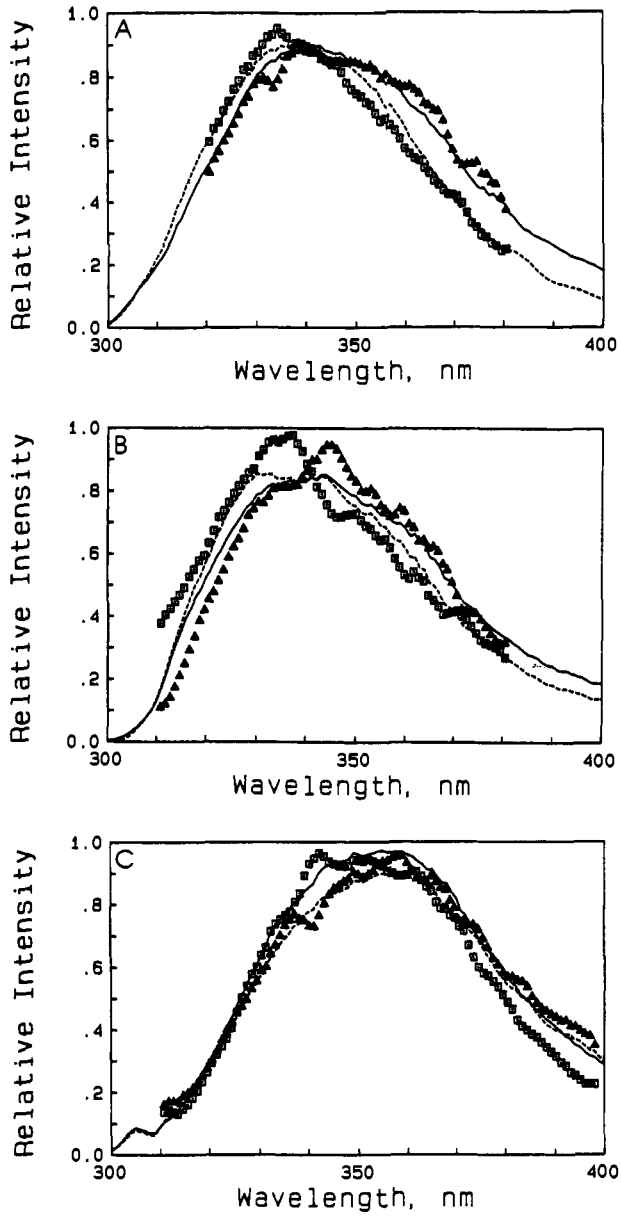

FIGURE 9: Comparison of the quenching decay-associated spectra with the middle- and long-lifetime components of the decay-associated spectra. Arginase was dialyzed versus 20 mM Hepes, pH 7.0, 200 mM NaCl, and 1 mM $MnCl_2$ (panel A); 20 mM Hepes, pH 7.0, and 200 mM NaCl (panel B); and 20 mM Hepes, pH 7.0, 200 mM NaCl, and 1 mM EDTA (panel C). The middle-lifetime component from the DAS is denoted by the dashed line and the long-lifetime component by the solid line. The QDAS associated with the smaller Stern–Volmer constant (shown in Table I) is denoted by the squares, and the QDAS associated with the larger Stern–Volmer constant is denoted by the triangles. Arginase concentration was 0.15 mg mL^{-1}.

Discussion

Arginase from *Saccharomyces cerevisiae* is a trimer of identical subunits (Duong et al., 1986; Eisenstein et al., 1986; Green et al., 1986) containing three tryptophans per polypeptide chain (Sumrada & Cooper, 1984). Time-resolved fluorescence and steady-state fluorescence were employed here to monitor the effects of removing the weakly bound catalytic Mn^{2+} as well as the tightly bound Zn^{2+}/Mn^{2+} on the environments of the tryptophans. Previously steady-state fluorescence experiments demonstrated large changes in emission spectra for native arginase, the enzyme in the absence of the catalytic Mn^{2+}, and the enzyme in the absence of both metals (Green et al., 1990b). These experiments suggested that there might also be changes in the DAS upon metal

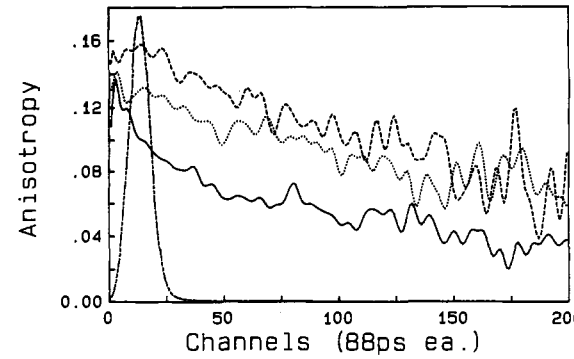

FIGURE 10: Anisotropy of arginase at room temperature as a function of metal ligation. Smoothed curves of the raw time-resolved anisotropy decay are shown for arginase dialyzed against 20 mM Hepes, pH 7.0, 200 mM NaCl, and 1 mM $MnCl_2$ (dashed line); 20 mM Hepes, pH 7.0, and 200 mM NaCl (dotted line); and 20 mM Hepes, pH 7.0, 200 mM NaCl, and 5 mM EDTA (solid line). A scaled lamp curve is given for reference (dashed–dotted line). Arginase concentration was 0.12 mg mL^{-1}.

removal. This, in turn, may shed more detail on the structural changes which result from removal of metal ions from the two affinity classes of metal ion binding sites.

Therefore, decay curves were taken throughout the emission spectra, and the DAS were obtained from global analysis (Beechem et al., 1983; Knutson et al., 1983) (Figure 1). Resolution of the total spectra for native arginase, arginase in the absence of the catalytic metal, and arginase in the presence of EDTA results in only two DAS. The third DAS is partially obscured by scattered excitation and other artifacts (Figure 3), even though a fourth component was included to correct for potential interference by light scattering. The reason that only two DAS can be resolved for three tryptophans is not clear. It may be that one or more tryptophans is internally quenched by a neighboring amino acid side chain or two or more tryptophans have very similar DAS (in terms of lifetimes and wavelength). Until the tryptophans are either chemically or genetically altered, this question will remain unanswered. The environments that *can* be observed provide definite spectral signatures that help to trace the structural changes.

As demonstrated in Figure 2, native arginase yields fluorescent components with lifetimes of 0.1, 1.2, and 4.0 ns. Removal of the catalytic Mn^{2+} results in almost no change in lifetimes from the native enzyme, with lifetimes of 0.1, 1.3, and 4.3 ns. A 30% increase in the steady-state fluorescence intensity upon removal of the weakly associated Mn^{2+} (Green et al., 1990b) without an increase in decay times suggests that Mn^{2+} may be acting to statically quench the intrinsic fluorescence of the enzyme. This could occur if removal of Mn^{2+} resulted in an increase in the extinction coefficient of the enzyme, or if Mn^{2+} holds the enzyme in a conformation where a population of amino acid side chains, capable of quenching, are in close proximity of the tryptophan. An alternative explanation is that tryptophans are known to nonspecifically bind divalent metal ions such as copper, nickel, and calcium (Ray Chen, personal communication) which quench tryptophan fluorescence. Although we cannot be sure if Mn^{2+} forms a weak association with these tryptophans, it is necessarily present in the native sample in such a molar excess that nonspecific adsorption seems likely. Alternatively, the bound, catalytic Mn^{2+} may itself be a static quencher.

Removal of the structural metal results in a large increase in the lifetimes of the fluorescent components to 0.2, 1.8, and 5.3 ns. This change in lifetimes suggests that the tryptophans move to a more polar environment in the apoenzyme, consistent

with the red-shift seen by steady-state and time-resolved fluorescence, and suggests unfolding of the enzyme (Green et al., 1990b). Lifetimes of approximately 2.0 and 5.0 ns are quite common for denatured proteins (Knutson et al., 1982b; Han et al., 1989), although the reason for this is not yet clear.

The DAS of the two major components also demonstrate little change upon removal of the catalytic Mn^{2+}, but a large red-shift for both fluorescent components upon removal of the structural metal (compare Figure 4A with Figure 4B). The fact that the two DAS become indistinguishable in the apoenzyme (Figure 5C) demonstrates that the tryptophans move to a similar environment, further indicative of at least partial unfolding.

A distribution-type fit of the data surface was also performed. The results of single-curve distribution (Gaussian) analyses were broad and unreliable, providing erratic drift with wavelength. Global linkage was tested as an alternative to reconstruct the entire surface. The results of this analysis, shown in Figure 6A for arginase with exogenous Mn^{2+}, demonstrate that the distribution of the lifetimes centers around the lifetimes that were previously obtained for DAS. Since the distribution is narrow, this indicates that the global fitting procedure accurately resolved lifetimes which probably represent a discrete species rather than the average of multiple species having similar lifetimes. This cannot be tested with a single wavelength alone. The unreliability of distribution fitting on single curves has been discussed previously (Knutson, 1987).

Previously, it has been shown that denaturation of liver alcohol dehydrogenase with acid resulted in its two DAS becoming red-shifted but retaining their distinct character (Knutson et al., 1982b), which demonstrated that the unfolding reaction was incomplete. The fact that the two DAS become superimposable when the structural metal is removed from arginase is surprising, considering that CD measurements reveal significant secondary structure in these monomers (Green et al., 1990a). Furthermore, the monomer that results from removal of structural metal is still competent to form trimer (Green et al., 1990b). The DAS suggest that even though the protein is only partially unfolded, the tryptophans are all exposed to solvent. This could occur if there are pockets of structure that become relaxed, allowing penetration by water molecules.

Since the DAS are identical in an enzyme that is only partially unfolded, one might expect that the tryptophans in this protein would be highly accessible to ionic quenchers. This, however, is not the case. Neither cesium nor iodide were efficient quenchers of tryptophan fluorescence in the apoenzyme (Figure 8B,C). There is a small component accessible to iodide (with a Stern–Volmer constant of 5.33, Table I), but this represents <12% of the total. Moreover, as metals are removed from the enzyme, the ability of cesium to quench actually diminished, decreasing from a Stern–Volmer constant of 0.24 in the native enzyme to 0.03 in the apoenzyme. The fact that there are a number of negative charges in the vicinity of at least one of the tryptophans (Sumrada & Cooper, 1984) makes this result even more surprising since the effectiveness of ionic quenchers is known to be modulated by charge groups in the vicinity of the tryptophans (Lehrer, 1971, 1978; Eftink & Ghiron, 1976, 1981). These results, taken together, suggest that some degree of secondary or tertiary structure must remain in the apoenzyme.

Acrylamide, on the other hand, is quite effective at quenching the fluorescence of all three samples. This is demonstrated both in Table I and by the Stern–Volmer plot in Figure 8A. Quenchability of the tryptophans in arginase to acrylamide, in all three states of metal ligation, can be resolved into two Stern–Volmer constants. The native enzyme had species that were 66% inaccessible and 34% accessible with Stern–Volmer constants of 0.88 and 4.35, respectively. Although it appears that the inactive enzyme had species that are less quenchable than the native enzyme, with Stern–Volmer constants of 0.56 and 2.44, the more available species represents 51% of the total. This could account for the similarity seen in the Stern–Volmer plots (Figure 8A). Both Stern–Volmer constants are higher for the enzyme that has been treated with EDTA, consistent with longer lifetimes of the tryptophans in this sample. This indicates that, since the tryptophans remain in the excited state for a longer period of time, they are more likely to be quenched by acrylamide. Moreover, the longer lifetimes are consistent with more polar environments around the tryptophans.

Since analysis of the acrylamide data resulted in two Stern–Volmer constants with considerable intensity, these results were compared to the DAS obtained previously for shape and wavelength maximum. The results of this comparison, as shown in Figure 9, demonstrate that the two trimeric forms of the enzyme have separate QDAS which overlap their DAS, while the enzyme that was treated with EDTA has QDAS that are similar, especially on the blue end of the spectra, which also correspond to its DAS. Just as the QDAS demonstrate that the tryptophans in the native and inactive enzyme are in distinct environments in a moderately hydrophobic portion of the protein, the QDAS for arginase treated with EDTA indicate that the tryptophans have moved into more polar environments, exhibiting similar characteristics. Moreover, since the QDAS correspond to the DAS, one can attempt to correlate net quenchability with lifetime. As expected, in all three cases, the more blue-shifted DAS, corresponding to the lower lifetime, correlates to the less quenchable species. The more highly quenched species corresponds to the species with the higher lifetime. This allowed the determination of apparent collision rates for all three samples (Table II). The native enzyme and the apoenzyme demonstrate *similar* collision rates of approximately 0.7 and 1.1 ns^{-1} M^{-1}. These numbers suggest that the only difference in the K_{sv} of the tryptophans in these samples is due to differences in the fluorescence lifetime. Since arginase in EDTA exhibits longer lifetimes, the tryptophans exhibit higher Stern–Volmer constants. Arginase in which only the catalytic Mn^{2+} has been removed, however, has collision rates that are half those seen in the other two samples. The reason for this is not clear. It is known that this sample displays different characteristics by CD (Green et al., 1990a), but whether these changes could account for the lower collision rates is not apparent, and must be taken as contradictory to the unchanged DAS.

To determine if the two DAS obtained by the global linkage were the result of differences in tryptophan fluorescence solely in the excited state, or of heterogeneity in the ground state, IEDAS were determined. These provide the effective absorbance spectrum linked to each DAS, and they indicate that at least part of the differences in the DAS are based upon differences in the tryptophan ground state. This is shown by the two IEDAS obtained both for the native enzyme and for the enzyme without the catalytic Mn^{2+} (Figure 7A,B, respectively). This approach, however, cannot be employed for the enzyme that has been treated with EDTA (Figure 7C) due to the two *indistinguishable* DAS; this leads to errors in matrix inversion. Thus, one cannot use this test for ground-state

heterogeneity of the tryptophans in the apoenzyme. Indistinguishable DAS, however, suggest a lack of heterogeneity in tryptophan environment. When IEDAS demonstrate two separate spectra, this indicates that the differences in the DAS cannot be entirely due to excited-state reactions such as solvent relaxation or energy transfer. Although such reactions may occur on the picosecond time scale, there are probably no slower (nanosecond) excited-state reactions occurring because the DAS for the short component (0.1 ns, native and inactive; 0.2 ns, EDTA) do *not* demonstrate a negative amplitude anywhere in the emission spectrum (Figure 3) (Knutson et al., 1990; Davenport et al., 1983, 1986). This suggests that even the short component is a result of ground-state heterogeneity. The presence of ground-state heterogeneity was expected because there are three tryptophans in the enzyme (Sumrada & Cooper, 1984). One would expect that the environments around these three residues are not identical.

Time-resolved anisotropy experiments demonstrate that the apoenzyme has a steady-state anisotropy half that of the two trimeric forms of the enzyme, indicating an increase in segmental mobility in the apoenzyme (Figure 10, Table III). As a control for the *G* factor, anisotropy determinations were also made on the steady-state fluorometer, which uses both polarizers for *G* factor correction. The results from that instrument were in good agreement with the time-resolved anisotropy (data not shown). Determination of the rotational correlation times demonstrates a fluorescent component with fast segmental mobility (<1.0 ns), suggesting that there is a portion of the protein that is free to wobble in the solvent. The amplitude of this species is only 20% in the native and inactive forms of the enzyme, while removal of the structural metal doubles this amplitude to 40%. All three samples also exhibit a dominant rotational correlation time of 20 ns. This value is rather small for a protein of 110000 daltons, and suggests that there is significant movement even in the native enzyme. Since a rotational correlation time of 20 ns suggests a molecular weight of approximately 40000 at room temperature, it is possible that there is a great deal of rotation at the interaction sites between the monomers (36700 daltons) such that the dominant species seen by the fluorometer is quasi-monomeric. Otherwise, the trimer may be generally flexible in other ways. The relative contribution (0–20%) of any 60-ns or longer component would be difficult to quantify since the lifetime of tryptophan emission gives us only a brief glimpse at the enzyme's motion.

Summary

Results presented here show the resolution of two DAS for the tryptophans in arginase. These tryptophanyl species are in distinct environments in the two trimeric forms of the enzyme, but are in similar environments in the apoenzyme. Quenching experiments with acrylamide provide similar results, while quenching with the ionic quenchers (cesium and iodide) demonstrate overall inaccessibility of the tryptophans, suggesting that the tryptophans are in a protected portion of the protein that retains structure even in the apoenzyme. IEDAS indicate that the reason for the heterogeneity in the DAS and QDAS is due to differences in the tryptophans originating in the ground state. These results corroborate those seen previously (Green et al., 1990a,b) that even though the removal of structural metal ions destabilizes the trimeric enzyme, yielding a significant amount of monomer, this dissociated form retains significant tertiary structure.

Acknowledgments

We thank Professor Jean-Marie Wiame and Dr. Francine Messenguy for generously providing *Saccharomyces cerevisiae* strain 02232i. Also, we thank Dr. Ludwig Brand and his laboratory for the use of their facilities and equipment to do the three-dimensional plots and Dr. Patrick J. Fleming for his many helpful discussions and support during this work.

Registry No. Mn, 7439-96-5; Zn, 7440-66-6; L-tryptophan, 73-22-3; arginase, 9000-96-8.

References

Alcala, J. R., Gratton, E., & Prendergast, F. G. (1987a) *Biophys. J. 51*, 587–596.

Alcala, J. R., Gratton, E., & Prendergast, F. G. (1987b) *Biophys. J. 51*, 597–604.

Alcala, J. R., Gratton, E., & Prendergast, F. G. (1987c) *Biophys. J. 51*, 925–936.

Badea, M. G., & Brand, L. (1979) *Methods Enzymol. 61*, 378–425.

Bechet, J., & Wiame, J.-M. (1965) *Biochem. Biophys. Res. Commun. 21*, 226–234.

Beechem, J. M., Knutson, J. R., Alexander Ross, J. B., Turner, B. W., & Brand, L. B. (1983) *Biochemistry 22*, 6054–6058.

Brand, L., Knutson, J. R., Davenport, L., Beechem, J. M., Dale, R. E., Walbridge, D. G., & Kowalczyzk, A. A. (1985) in *Spectroscopy and the Dynamics of Molecular Biological Systems* (Bayley, P. M., & Dale, R. E., Eds.) pp 259–305, Academic Press, London.

Carvajal, J., Venegas, A., Oestricher, G., & Plaza, M. (1971) *Biochim. Biophys. Acta 250*, 437–442.

Carvajal, N., Martinez, J., & Fernandez, M. (1977) *Biochim. Biophys. Acta 481*, 177–183.

Carvajal, N., Martinez, J., Montes de Oca, F., Rodriguez, J., & Fernandez, M. (1978) *Biochim. Biophys. Acta 527*, 1–7.

Davenport, L., Knutson, J. R., & Brand, L. (1983) *Biophys. J. 41*, 373a.

Davenport, L. Knutson, J. R., & Brand, L. (1986) *Biochemistry 25*, 1186–1195.

Duong, L. T., Eisenstein, E., Green, S. M., Ornberg, R. L., & Hensley, P. (1986) *J. Biol. Chem. 261*, 12807–12813.

Eftink, M. R., & Ghiron, C. A. (1976) *Biochemistry 15*, 672–680.

Eftink, M. R., & Ghiron, C. A. (1981) *Anal. Biochem. 114*, 199–227.

Eisenstein, E. (1985) Ph.D. Thesis, Georgetown University, Washington, DC.

Eisenstein, E., & Hensley, P. (1986) *J. Biol. Chem. 261*, 6192–6200.

Eisenstein, E., Osborne, J. C., Jr., Chaiken, I. M., & Hensley, P. (1984) *J. Biol. Chem. 259*, 5139–5145.

Eisenstein, E., Duong, L. T., Ornberg, R. L., Osborne, J. C., Jr., & Hensley, P. (1986) *J. Biol. Chem. 261*, 12814–12819.

Green, S. M. (1989) *Biophys. J. 55*, 532a.

Green, S. M., McPhie, P., & Hensley, P. (1986) *Fed. Proc. 45*, 1920a.

Green, S. M., Knutson, J. R., & Hensley, P. (1988) *J. Cell. Biol. 107*, 200a.

Green, S. M., Eisenstein, E., McPhie, P., & Hensley, P. (1990a) *J. Biol. Chem. 265*, 1601–1607.

Green, S. M., Ginsburg, A., Lewis, M. S., & Hensley, P. (1990b) *J. Biol. Chem.* (submitted for publication).

Han, M., Knutson, J., Kim, S., Fisher, M., Cyran, F., & Ginsburg, A. (1989) *Biophys. J. 55*, 120a.

Hensley, P. (1988) *Curr. Top. Cell. Regul. 29*, 35–75.

Hirsch-Kolb, H., & Greenberg, D. M. (1986) *J. Biol. Chem. 243*, 6123–6129.

Hirsch-Kolb, H., Heine, J. P., Kolb, H. J., & Greenberg, D. M. (1970) *Comp. Biochem. Physiol. 37*, 345–359.

Hirsch-Kolb, H., Kolb, H. J., & Greenberg, D. M. (1971) *J. Biol. Chem. 246*, 395-401.
Knutson, J. R. (1987) *Biophys. J. 51*, 285a.
Knutson, J. R. (1988) *Proc. SPIE—Int. Soc. Opt. Eng. 909*, 51-60.
Knutson, J. R., Baker, S. H., Cappucino, A. G., Walbridge, D. W., & Brand, L. (1982a) *Photochem. Photobiol. 37*, S21.
Knutson, J. R., Walbridge, D. G., & Brand, L. (1982b) *Biochemistry 21*, 4671-4679.
Knutson, J. R., Beechem, J. M., & Brand, L. (1983) *Chem. Phys. Lett. 102*, 501-507.
Knutson, J. R., Chen, R. F., Scott, C. S., & Bowman, R. L. (1984) *Photochem. Photobiol. 41*, 78a.
Knutson, J. R., Davenport, L., Beechem, J., Walbridge, D., Ameloot, M., & Brand, L. (1990) *NATO ASI Ser.* (in press).
Lehrer, S. S. (1971) *Biochemistry 10*, 3254-3263.
Lehrer, S. S. (1978) *Methods Enzymol. 49*, 222-236.
Messenguy, F., & Wiame, J.-M. (1969) *FEBS Lett. 3*, 47-49.
Penninckx, M. (1975) *Eur. J. Biochem. 58*, 533-538.
Penninckx, M., & Wiame, J.-M. (1976) *J. Mol. Biol. 104*, 819-831.
Penninckx, M., Simon, J.-P., & Wiame, J.-M. (1974) *Eur. J. Biochem. 49*, 429-442.
Sackett, D. L., Knutson, J. R., & Wolff, J. (1990) *J. Biol. Chem.* (in press).
Stewart, J. A., & Caron, H. (1977) *J. Neurochem. 29*, 657-663.
Sumrada, R. A., & Cooper, T. G. (1984) *J. Bacteriol. 160*, 1078-1087.
Ville-Brietburd, F., & Orth, G. (1972) *J. Biol. Chem. 247*, 1227-1235.
Wiame, J.-M. (1971) *Curr. Top. Cell. Regul. 4*, 1-38.

Chemical Modification of Tryptophan Residues and Stability Changes in Proteins

Toshihide Okajima, Yasushi Kawata,[‡] and Kozo Hamaguchi*
Department of Biology, Faculty of Science, Osaka University, Toyonaka, Osaka 560, Japan
Received December 7, 1989; Revised Manuscript Received May 24, 1990

ABSTRACT: The role of tryptophan residues in the stability of proteins was studied by ozone oxidation, which causes a small change in the tryptophan side chain. Trp 187 of the constant fragment of a type λ immunoglobulin light chain, Trp 59 of ribonuclease T1, and Trp 62 of hen egg white lysozyme were oxidized specifically by ozone to *N'*-formylkynurenine or kynurenine. Judging from their circular dichroic and fluorescence spectra, these modified proteins were found to be the same as those of the respective intact proteins. However, even the slight modification of a single tryptophan residue produced a large decrease in the stability of these proteins to guanidine hydrochloride and heat. The smaller the extent of exposure of the tryptophan residue, the greater the effect of the modification on the stability. The formal kinetic mechanism of unfolding and refolding by guanidine hydrochloride of the C_L fragment was not altered by tryptophan oxidation, but the rate constants for unfolding and refolding changed. The thermal unfolding transitions were analyzed to obtain the thermodynamic parameters. The enthalpy and entropy changes for the modified proteins were larger than the respective values for the intact proteins.

Site-specific modification by synthetic and recombinant DNA technology has recently been used to clarify the structure, stability, and function of proteins. The chemical modification method has also been used so far mainly for identifying the functional groups of proteins. However, the structure and stability of such chemically modified proteins have not been studied in detail.

In the present studies, we examined the role of tryptophan residues in the structure and stability of proteins. For this purpose, we employed ozone oxidation to modify the tryptophan residue. No other amino acid closely resembles tryptophan. It is thus impossible to make a small change in a tryptophan side chain by site-directed mutagenesis, and it can only be achieved by using the chemical modification. Ozone oxidation modifies the tryptophan residue to *N'*-formylkynurenine (NFK),[1] which is converted to kynurenine (Kyn) by freezing in acid (Kuroda et al., 1975; Tamaoki et al., 1978; Yamasaki et al., 1979; Teshima et al., 1980; Fukunaga et al., 1982a,b):

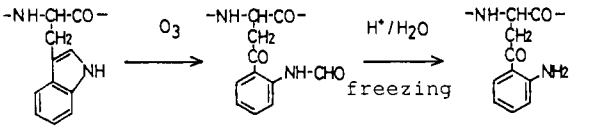

Trp NFK Kyn

X-ray crystallographic analysis of *N*-acetylkynurenine crystals (Kennard et al., 1979) has shown that the carbonyl oxygen is hydrogen-bonded to the aromatic amino group at

[‡] Present address: Department of Chemistry, Faculty of Science, Kyoto University, Sakyo-ku, Kyoto 606, Japan.

[1] Abbreviations: CD, circular dichroism; Gdn-HCl, guanidine hydrochloride; SDS, sodium dodecyl sulfate; Tris, tris(hydroxymethyl)-aminomethane; HPLC, high-performance liquid chromatography; C_L-(109-212), C_L fragment corresponding to sequence 109-212; NFK, *N'*-formylkynurenine; Kyn, kynurenine; NFK 187-C_L, C_L fragment in which Trp 187 is modified to NFK; Kyn 187-C_L, C_L fragment in which Trp 187 is modified to Kyn; NFK (150, 187)-C_L, C_L fragment in which Trp 150 and Trp 187 are modified to NFK; Kyn (150, 187)-C_L, C_L fragment in which Trp 150 and Trp 187 are modified to Kyn; NFK 59-RNase T1, ribonuclease T1 in which Trp 59 is modified to NFK; Kyn 59-RNase T1, ribonuclease T1 in which Trp 59 is modified to Kyn; NFK 62-lysozyme, hen egg white lysozyme in which Trp 62 is modified to NFK; Kyn 62-lysozyme, hen egg white lysozyme in which Trp 62 is modified to Kyn.

0006-2960/90/0429-9168$02.50/0